Electronic Supporting Information

(ESI)

Cellular uptake of covalent and non-covalent DNA nanostructures with different size and geometry

Sofia Raniolo[1, 4], Stefano Croce[2], Rasmus P. Thomsen[3], Anders H. Okholm[3*], Valeria Unida[4], Federico Iacovelli[4], Antonio Manetto[5], Jørgen Kjems[3], Alessandro Desideri[4], Silvia Biocca[1§],

[1]Department of Systems Medicine, University of Rome Tor Vergata, Via Montpellier 1, 00133, Rome, Italy.

[2]Baseclick GmbH, Floriansbogen 2-4, 82061 Neuried, Germany

[3]Interdisciplinary Nanoscience Center (iNANO), Aarhus University, Aarhus , Denmark.

[4]Department of Biology, University of Rome Tor Vergata, Via della Ricerca Scientifica 1, 00133, Rome, Italy.

[5]Metabion, Gesellschaft für angewandte Biotechnologie mbH, 82152 Planegg, Germany

[*]*Present address:* Arla Innovation Centre, Arla Foods amba, Agro Food Park 19, 8200, Aarhus N, Denmark

[§]*Correspondence to:* biocca@med.uniroma2.it

S1. Sequences of oligonucleotides used for the assembly of non-covalent and covalent DNA tetrahedra

Unmodified oligonucleotides were HPLC purified and purchased from Sigma Aldrich. The sequences of the oligonucleotides are reported in Table S1. The 5' of each oligonucleotide is phosphorylated. TTTTT represents a short non-pairing spacer inserted within the strands as a DNA junction at each vertex of the assembled 3D structure. $OL3_{BIO}$ has a biotin tetra-ethylene-glycol molecule (BtndT) at the T represented in red.

Oligo	Sequences
1	5'-P-CCACGGCGCTTTTTTTGCTGCTCCTTCCTTATCCTTTTTTTCGTCGACCGCCCAATTACTTTTTTTCCACTAATT-3'
2	5'-P-ACTCTCCCGTTTTTTTGACGACGCGCATTCCAGCTTTTTTTGTAATTGGGCGGTCGACGTTTTTTTGGCAAACCC-3'
3_{BIO}	5'-P-CGCGTCGTCTTTTTTTGTAAGTATGATTGTAGGGTTTTTTGCGCCGTGGAATTAGTGGTTTTTTTGCTGGAATG -3'
4	5'-P-CATACTTACTTTTTTTCGGGAGAGTGGGTTTGCCTTTTTTTGGAGTAAGGAAGGAGCAGCTTTTTTTCCCTACAAT-3'

Table S1. Sequences of the oligonucleotides used for the assembly of Bio-DNA tetrahedra. In red is depicted the biotinylated T in $OL3_{BIO}$.

S2. Sequences of oligonucleotides used for the assembly of non-covalent and covalent DNA chainmails

5'-Azide, 3'-Alkyne oligonucleotides were HPLC purified and purchased from Metabion, Germany. The sequences of the oligonucleotides are reported in Table S2. After folding, the oligonucleotides form a 6-helix bundle in which the 5' and 3' click functionalities are pre-organized and ready to react efficiently in presence of Cu(I).

Oligo	Sequences
hct-ODN1	5'-ZAAAACGCTAAGCCACCTTXAGATCCAAXCAGATACTCGGT-3'
ct-ODN2	5'-ZGGTCGTGCGGACTGTCGAACACCAACGATGCCTGATAGAAGX-3'
ct-ODN3	5'-ZGCGTGGCAATAGCCATAAATTCATACATAACGGCGCCAGACX-3'
ct-ODN4	5'-ZTTTCAAGACCAGCACTTGTATGGCGTAGGGCGGGTTTAGCGX-3'
ct-ODN5	5'-ZGGATCTAAAGGACTTCTATCAAAGACGGGACGACTCCGGGAX-3'
ct-ODN6	5'-ZGGCATCGTTGGAGTCTGGCGCACGACTTCGATTTCGGATCCX-3'
bct-ODN1	5'-ZCGTTATGTATGACGCTAAACCTTGCAATGACTGAACTCGAAX-3'
ct-ODN8	5'-ZCGCCCTACGCCAAAAAAGATGGGAGCTX-3'
hct-ODN2	5'-ZCGTTAXGTATGACGCTAAACCTTGCAATGACTGAACTCGAAT-3'
bct-ODN2	5'-ZGTCCCGTCTTAGGATCCGAAAGCCAXAATATATCGAGACGGX-3'
ct-ODN11	5'-ZTCGAAGTCGTATTCGAGTTCAAATGTCTATGCGATGCAGCAX-3'
ct-ODN12	5'-ZGTCATTGCAAAAGCTCCCATCATTTAATGTCGTTTACAGTAX-3'
ct-ODN13	5'-ZGATCAGCAGCGACCGTCTCGACTGCAGAAATAGGACCCCCAX-3'
ct-ODN14	5'-ZTATATTATGGCATGCTGCATCTTCCTGGCATGGCTGAATTCX-3'
bct-ODN3	5'-ZGCATAGACATTATACXGTAAAACCTTACGTAACTTACAGCCX-3'
ct-ODN16	5'-ZCGACATTAAATAAAAAAGATGAGTATTX-3'
hct-ODN3	5'-ZAAAATGGGGGTCCTCGAGGCGAAACAAXCAGATACTCGGT-3'
bct-ODN4	5'-ZATTTCXGCAGAGAATTCAGCCTATTCACATAGGCGAAGGCTX-3'
ct-ODN19	5'-ZATGCCAGGAAAGGCTGTAAGTTGCATCATGGGGGTCCTCAAX-3'
ct-ODN19	5'-ZTACGTAAGGTAAATACTCATCCCTGAGTGATCCATGACCCTX-3'
ct-ODN21	5'-ZGTTTCGCCTCGAAGCCTTCGCCCGCACGACCTGGCTTAGCGX-3'
ct-ODN22	5'-ZCTATGTGAATAATTGAGGACCATTGCCACGCTGTTCGACAGX-3'
bct-ODN5	5'-ZCCCATGATGCAAAGGGTCATGGGTCTTGAAAAATTTAXGGCX-3'
ct-ODN24	5'-ZGATCACTCAGGAAAAAAATACAAGTGCX-3'

Table S2. Sequences of the oligonucleotides used for the assembly of DNA chainmails. Z: Azide; X: Alkyne

S3. Click reaction

Starting from the original design previously described[1], eight click tail oligonucleotides (ODN) were replaced with 5 bct-ODNs having the same sequence with an extra alkyne moiety and three hct-ODNs having the same sequence with an extra strand carrying an optional modification. The click reaction was performed using 40 µl of the solution containing the folded nanostructures (0.5 µM) where it was added 6 mg of the heterogenous Cu catalyst, 10 µL of Cu ligand Tris (benzyltriazolylmethyl) amine (THPTA baseclick GmbH) 0,1 M and 1 µL of Biotin-Peg3-Azide (baseclick GmbH) 1 mM. The solution was then incubated at 32 °C for 5 hours gently mixing at 200 rpm. The mixture was then transferred in a fresh vial and the Cu catalyst discharged. The sample was analyzed without any further purification step. For cell experiments, the chainmails were purified *via* EtOH precipitation.

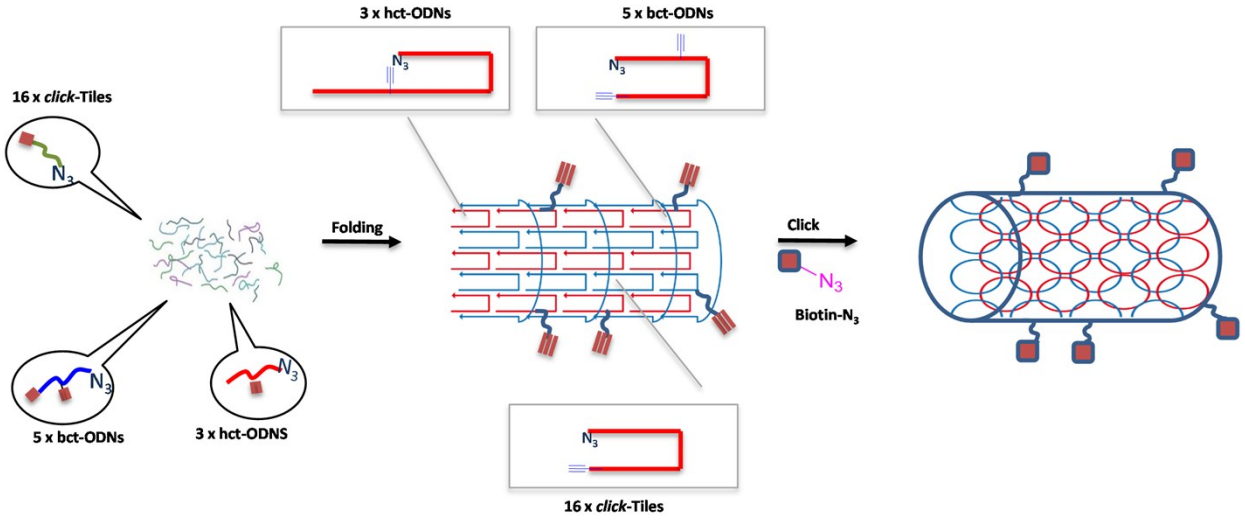

Figure S1. Schematic representation of the DNA chainmail functionalization. After the folding reaction *via* one-pot click reaction, it is possible to close the click tails leading to chainmail formation and, at the same time, to labeling the structure with biotin. Nomenclature: bct-ODN = body (functional) click tile; hct-ODN = head (functional) click tile.

S4. Stability of square box origami structures in 10%FBS

Square box origami (SBO) were incubated at 37°C with 10% fetal bovine serum (FBS) for different time intervals, as indicated. After incubation, SBO samples were run in 1% agarose gel to examine the structural integrity. The presence of 32 biotin molecules allows the detection of SBO through a streptavidin-HRP-biotin reaction in DNA blots.

As shown in Figure S4, SBO structures start to lose their integrity between 3 and 24 h. Notably, the SBO loss of structure and degradation causes an increase in the intensity of the signal of the band detected by the streptavidin-biotin reaction in DNA blot (lane 4) as observed for RO (Figure 2, lanes 4 and 5).

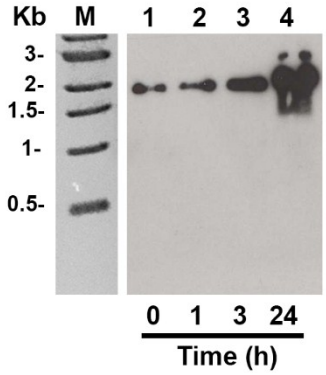

Figure S2. Stability of biotinylated SBO in serum. DNA blot analysis of SBO incubated with 10% FBS. 20 ng of SBO before incubation with serum proteins (time 0) are shown in lane 1. Incubation times are indicated under the gel.

S5. Membrane LOX-1 receptors visualized with Mab anti-V5 IgG

COS cells were plated on poly-L-lysine coated glass slides and then transfected with pEF/V5-LOX-1, a plasmid encoding for the full-length LOX-1 receptor containing a V5-tag at the C-terminus (LOX-1-V5). After 24 hours from transfection, cells were incubated with Mab anti-V5 for 1 h at 4°C for visualizing LOX-1-V5 receptors expressed at the cell surface (Figure S5). Cells were washed in PBS, fixed in 4% paraformaldehyde and neutralized with $NaBH_4$. Rhodamine Red-X-conjugated AffiniPure donkey anti-mouse IgG was used as secondary antibody and nuclei were stained with DAPI. In Figure S5 LOX-1 receptors are represented by red fluorescent intense dots, indicating that the receptors localize on the outer surface of the plasma membranes. It is worth noting that within transfected LOX-1 cells some cells (white arrows) do not express LOX-1 according to the transfection efficiency of 40% and do not show any red membrane fluorescence around the blue nuclei.

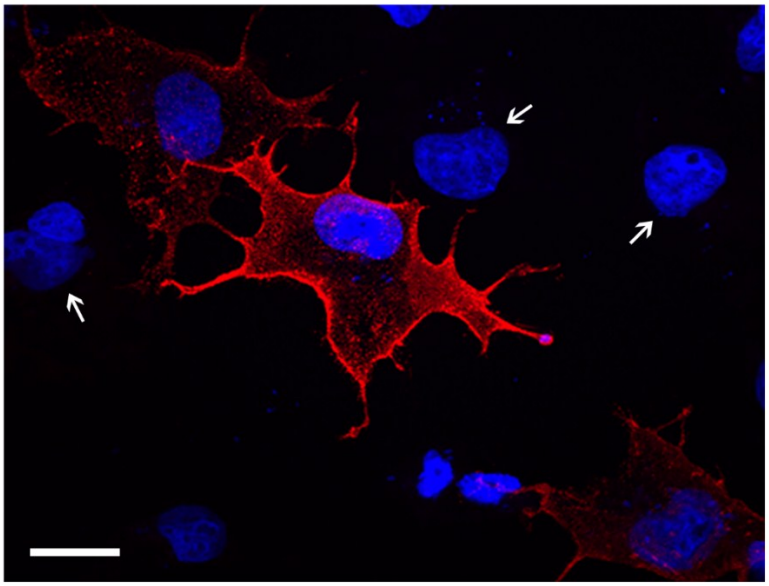

Figure S3. Confocal analysis of LOX-1-expressing COS cells incubated with Mab anti-V5 for 1 h at 4°C. White arrows indicate some not-transfected cells. Images were obtained with a laser confocal fluorescence microscope Olympus FV1000 at 60X magnification and processed by IMARIS software. Scale bar: 20 μm.

S6. Co-detection of LOX-1 receptors and SBO structures in LOX-1 expressing COS cells.

For the binding experiment, COS cells were transfected with pEF/V5-LOX-1 plasmid and, after 24 h, incubated with biotin-labeled SBO origami (4 µg/mL) for 1 h at 4°C, fixed in 4% paraformaldehyde and neutralized with $NaBH_4$. Biotinylated SBO were detected with streptavidin-FITC (Jackson) and nuclei stained with DAPI (Invitrogen). In Figure S6, panels a and b, SBO origami are detected as green fluorescent intense dots, indicating that they localize on the plasma membrane surface.

For co-detection of LOX-1 receptors and SBO structures, LOX-1-transfected COS cells were incubated with biotinylated SBO (4 µg/mL) for 1 h at 37°C, fixed with 4% paraformaldehyde and permeabilized with Tris-HCl 0.1M pH 7.6/Triton 0,1%, for allowing the detection of both internalized structures and intracellular LOX-1 receptors. Cells were stained with anti-V5 antibodies and streptavidin−FITC, for visualizing LOX-1 receptors and biotinylated SBO respectively and with DAPI for localizing the nuclei. Figure S6 shows representative confocal images in which unequivocally LOX-1-expressing cells (red fluorescence, panel c) have internalized SBO structures (green fluorescence, panels d and e).

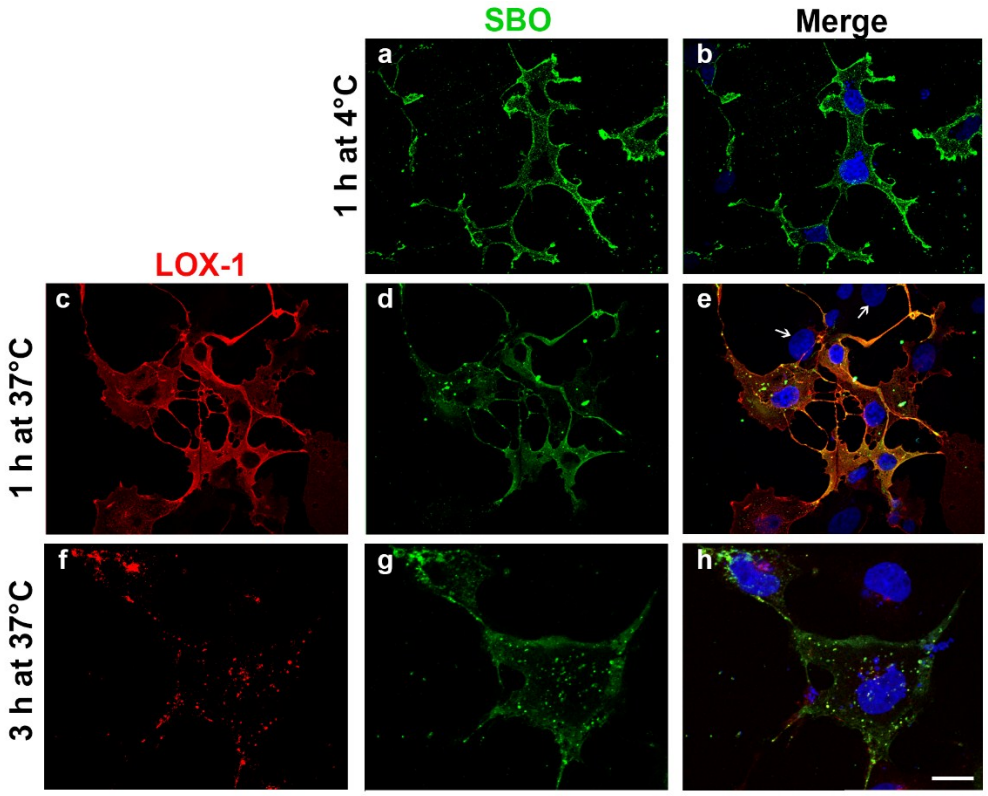

Figure S4. Binding of SBO to LOX-1-expressing COS cells and co-detection of LOX-1 receptors and SBO structures. Confocal analysis of LOX-1-expressing COS cells incubated with biotinylated SBO for 1 h at 4°C (panels a and b) and with biotinylated SBO for 1 h at 37°C (panels c, d, and e). SBO were detected by using streptavidin−FITC (green) and LOX-1 receptors were visualized using anti-V5 antibody (red). Nuclei were stained with DAPI (blue). White arrows show not-transfected cells. Images were obtained with a laser confocal fluorescence microscope Olympus FV1000 at 60X magnification and processed by IMARIS software. Scale bar: 20 µm.

S7. Confocal analysis of biotinylated DNS internalized in not-transfected COS cells compared to LOX-1 transfected cells.

In order to demonstrate a specific binding between DNS and LOX-1 receptors, we have performed uptake experiments on LOX-1 transfected (COS-LOX-1) or not-transfected (COS nt) COS cells. In detail, cells were incubated with biotinylated DNS (10 µg/mL for TD and CM and 4 µg/mL for RO) for 1 h at 37°C, fixed with 4% paraformaldehyde and permeabilized with Tris-HCl 0.1M pH 7.6/Triton 0,1%, for allowing the detection of the internalized structures. Cells were stained with streptavidin−FITC for visualizing biotinylated DNS and with DAPI for localizing the nuclei. Figure S7 shows representative confocal analysis in which LOX-1-expressing cells (panel a, c, and e) have internalized biotinylated DNS while no green fluorescence was detectable inside the COS nt cells (panels b, d, and f) for any of the DNS tested, indicating a LOX-1-dependent cellular uptake of DNS.

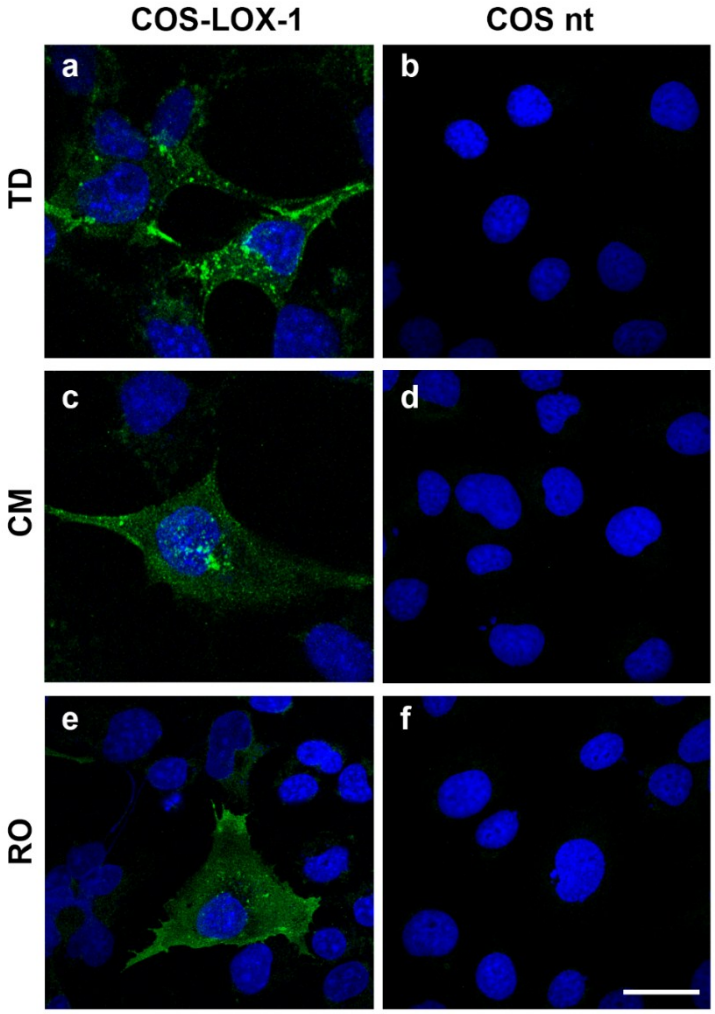

Figure S5. Representative confocal images of DNS uptake in COS cells. COS-LOX-1 (panels a, c, and e) and COS nt cells (panels b, d, and f) were incubated for 1 h at 37°C with biotinylated TD, CM, and RO. Biotinylated DNS were detected with streptavidin-FITC and nuclei were blue stained

with DAPI. Images were obtained with a laser confocal fluorescence microscope Olympus FV1000 at 60X magnification and processed by IMARIS software. Scale bar, 20 μm.

S8. Competition assays.

To study the specificity of LOX-1 recognition, two competition binding assays were performed, one in the presence of 10 times more concentrated single stranded oligonucleotide and one in the presence of non-biotinylated DNS. Figure S8 shows representative confocal images of the competition assays performed by incubating LOX-1 expressing cells with 144 nM biotinylated tetrahedral nanocages (Bio-TD) in the absence (panel a), in the presence of 1,4 μM 29 nt single-stranded oligonucleotide with random sequence (10x oligo, panel b) and in the presence of 1,4 μM of non-biotinylated (10x TD) (panel c). In detail, 24h after transfection, COS cells were simultaneously incubated with Bio-TD and 10x oligo or 10x TD for 1 h at 4°C. Cells were then fixed in 4% paraformaldehyde and neutralized with NaBH4. Biotinylated TD were detected with streptavidin-FITC (Jackson) and nuclei stained with DAPI (Invitrogen). As shown in Figure S8, panel b, the presence of 10x oligo does not impair Bio-TD binding to LOX-1 expressing cells. Of note, 10-fold excess of not-biotinylated fully assembled TD almost completely abolishes TD binding to LOX-1 (panel c), indicating the specificity of the binding.

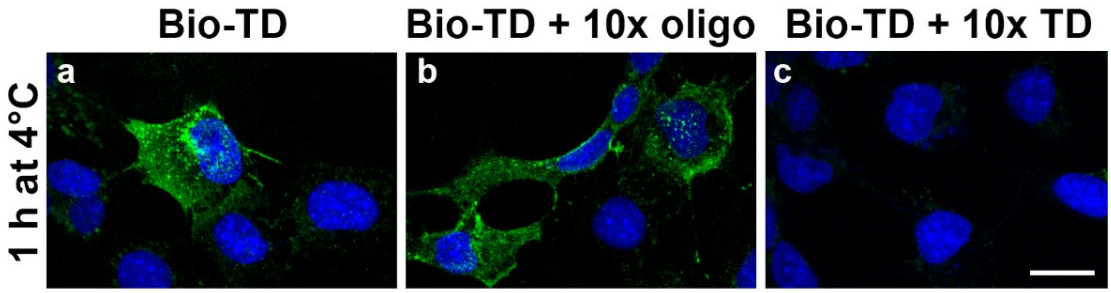

Figure S6. Competition assays. LOX-1 transfected COS cells were incubated with 144 nM Bio-TD (panel a) in the simultaneous presence of 10-fold excess of a single-stranded oligonucleotide (panel b) or non-biotinylated TD (panel c) for 1 h at 4°C. Biotinylated TD were detected with streptavidin-FITC and nuclei are blue stained with DAPI. Images were obtained with a laser confocal fluorescence microscope Olympus FV1000 at 60X magnification and processed by IMARIS software. Scale bar, 20 μm.

S9. TD and CM internalization in not-transfected COS cells compared to LOX-1 transfected cells.

Not expressing (-) and LOX-1 expressing (+) COS cells were incubated with 6 μg/mL of biotinylated TD and CM for 1 h at 37 °C. After incubation, cells were lysed, centrifuged and supernatants digested with proteinase K for removing the bound proteins that surround the surface of DNS. Samples were analyzed by DNA blot. Figure S9 shows the amount of tetrahedral (TD, panel A) and chainmail (CM, panel B) internalized by not-transfected (-) compared to LOX-1 transfected COS cells (+). The amount of DNS found in not-transfected cells was calculated by densitometric analysis. After 1 h of incubation at 37°C, not-transfected COS cells internalize a very low amount of TD and CM that have been quantified to be 4.6±0.7 ng/10^{6cells} and 8.4±0.9 ng/10^{6cells}, respectively. At the same time of incubation, LOX-1-expressing COS cells internalize 140 ± 33ng/10^{6cells} of TD and 261± 69 ng/10^{6cells} of CM, confirming that LOX-1-mediated uptake leads to an increase of about 30-fold in the amount of internalized DNS.

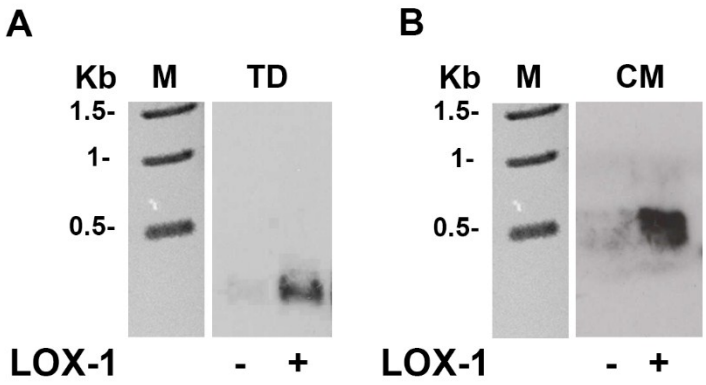

Figure S7. Representative DNA blots of cell extracts obtained from COS cells expressing (+) or not expressing (-) LOX-1 receptor incubated with TD (A) and CM (B). Biotinylated DNS were detected with streptavidin-HRP and visualized by enhanced chemiluminescence.

S10. Stability of non-covalently-linked OD structures in cells.

Non covalently-linked DNS are more unstable in biological fluids. For evaluating their stability inside cells, we incubated biotinylated non covalent octahedral nanocages (ncOD) (6 μg/mL) with LOX-1-transfected COS cells for 3 and 18 h at 37 °C, we purified them from cell lysates and conditioned media, treated with proteinase K (100 μg/mL) for 1 h at 37°C and run on 1% agarose gel in TBE (Tris-Cl 89 mM pH 8, boric acid 89 mM, EDTA 2mM). A representative DNA blots is shown in Figure S10A. Lanes 1 and 4 show the electrophoretic mobility of ncOD before incubation with cells (time 0). After 3 h of incubation, intact ncOD structures are barely detectable in cells lysates (lane 2) and, after 18 h of incubation, only a smear is visible in cell lysates indicating that the nanostructures have been degraded (lane 3). Notably, the analysis of the ncOD in the conditional medium at the same time points (lanes 5 and 6), shows that after 18 h the ncOD structures are completely degraded, confirming their lower stability, when compared to the covalent DNA nanostructures.

For evaluating whether ncOD undergoes disassembly or degradation at the level of the plasma membrane, biotinylated ncOD (6 μg/mL) were incubated with LOX-1-transfected COS cells for 1 h at 4 °C, for avoiding cell internalization and analyzing the ncOD bound to the cell surface. Analysis of the purified ncOD by DNA blot indicates that, despite the low amount of membrane bound ncOD (Figure S10B, lane 2), only a single product is present in the gel with a mobility comparable to the input (lane 1), indicating that binding of ncOD to the receptor is not inducing disassembly or degradation of the structures.

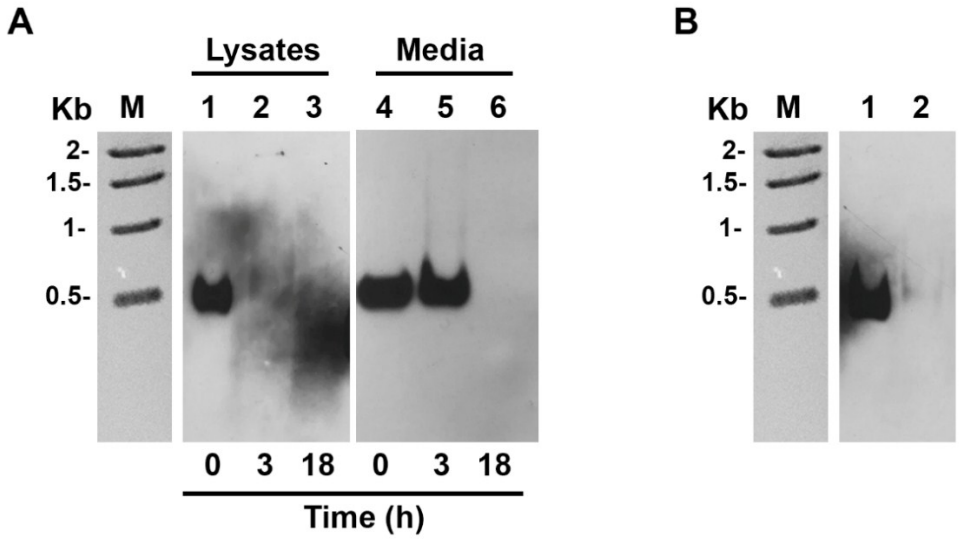

Figure S8. LOX-1-mediated uptake of ncOD and their binding to cells. (A) Representative DNA blots of lysates and conditioned media from LOX-1-transfected cells incubated with biotinylated ncOD for different times at 37 °C, as indicated. (B) Representative DNA blot of lysates of LOX-1-transfected cells incubated with biotinylated ncOD for 1 h at 4°C. NcOD were detected with streptavidin-HRP.

S11. Stability of SBO structures in cells.

Biotinylated SBO (6 μg/mL) were incubated with LOX-1-transfected COS cells for 1, 3 and 18 h at 37 °C, treated with proteinase K (100 μg/mL) for 1 h at 37°C and run on 1% agarose gel in TBE (Tris-Cl 89 mM pH 8, boric acid 89 mM, EDTA 2mM), supplemented with 6.25 mM $MgCl_2$.

DNA blots were visualized by using streptavidin-HRP. Lane 4 in Figure S11 shows the electrophoretic mobility of SBO before incubation with cells (input). Purified SBO, after incubation with cells, run with a lower electrophoretic mobility compared to the input (Figure S11, compare lanes 1, 2 and lane 3 with lane 4) and a DNA product with a lower molecular weight, corresponding to 1 kb, is detected inside cells, as reported for RO (Figure 6, lanes 2, 3 and 4).

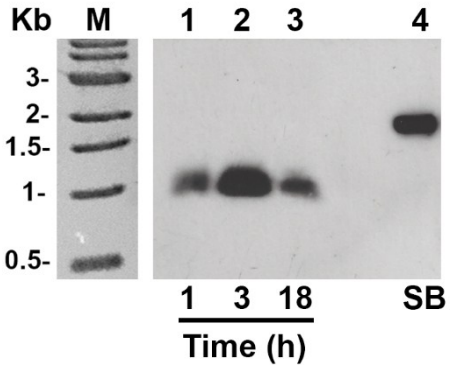

Figure S9. LOX-1-mediated uptake of SBO origami in COS cells. Representative DNA blot of cell extracts derived from LOX-1-transfected COS cells incubated with biotinylated SBO for 1, 3 and 18 h at 37 °C.

References:

1. V. Cassinelli, B. Oberleitner, J. Sobotta, P. Nickels, G. Grossi, S. Kempter, T. Frischmuth, T. Liedl, A. Manetto. Angew Chem Int Ed Engl. 2015, **54**, 7795-8.